



Mechanism regulating the inhibition of lung cancer A549 cell proliferation and structural analysis of the polysaccharide *Lycium barbarum*

Wenjin Ma^{a,d,1}, Yanbing Zhou^{b,1}, Wenjin Lou^c, Bo Wang^b, Bing Li^b, Xiaofen Liu^d, Jiajun Yang^d, Bo Yang^d, Jianfei Liu^{a,**}, Duolong Di^{a,*}

^a CAS Key Laboratory of Chemistry of Northwestern Plant Resources and Key Laboratory for Natural Medicine of Gansu Province, Lanzhou Institute of Chemical Physics, Chinese Academy of Sciences, Lanzhou, 730000, China

^b The Institute of Gansu Province Light Industrial Scientific Research, Lanzhou, 730000, China

^c Gansu Provincial Academic Industrial for Medical Research, Lanzhou, 730000, China

^d School of Life Science and Engineering, Lanzhou University of Technology, Gansu Province, Lanzhou, 730050, China

ARTICLE INFO

Keywords:

Lycium barbarum polysaccharide
Lung cancer cell
Apoptosis
Cell cycle
Structural analysis

ABSTRACT

The water-soluble polysaccharide LBP-1 was isolated and characterized from *Lycium barbarum* L. LBP-1 was mainly composed of arabinose, galactose, glucose, xylose, mannose at a molar ratio of 37.53: 28.08: 14.72: 7.83: 4.50, respectively. Based on nuclear magnetic resonance (NMR) and methylation analysis, the backbone of LBP-1 was speculated in the α -L-Ara(1 \rightarrow [5- α -L-Ara(1 \rightarrow 3)- β -D-Galp-(1 \rightarrow]n \rightarrow 4)- α -D-Galp-(1[\rightarrow 5- α -L-Ara(1)n[\rightarrow 6)- β -D-Galp-(1 \rightarrow 4)- β -D-Galp-(1 \rightarrow]n), and the side chains of LBP-1 were in the α -L-Ara(1 \rightarrow 3)- β -D-Galp-(1 \rightarrow 6) position. These results showed that LBP-1 inhibited the growth of cancer A549 cells through cell cycle arrest and apoptosis, with an IC50 value of 42.5 μ g/mL. In addition, LBP-1 altered the expression of Cyclin D1, Cyclin D3, and CDK 2, thus blocking the cell cycle in G0/G1 phase, reducing cell migration, and regulating the PI3K/Akt/mTOR signaling pathway to induce apoptosis.

1. Introduction

Lung cancer is one of the most common cancers worldwide, caused by the imbalance of cell proliferation and apoptosis. It has high incidence and morbidity rates, posing a serious threat to human life and health (Brody, 2014; Mattern & Volm, 2004). At present, traditional lung cancer treatments include surgical resection, radiotherapy, and chemotherapy. However, chemoradiotherapy causes serious side effects. Therefore, it is critical to discover natural anti-lung cancer drugs with high efficacy, low toxicity, and minimal side effects (Duma et al., 2019).

In recent years, plant polysaccharides have been identified as potential new anti-tumor drug resources (Jiao et al., 2016). For instance, *Astragalus* polysaccharide can effectively alleviate cancer-related fatigue in patients (Huang et al., 2019); *Ganoderma lucidum* polysaccharide promotes cell apoptosis, thereby inhibiting the proliferation of intestinal cancer cells (Pan et al., 2019); *Polyporus umbellatus* polysaccharide (PUPS) enhances the immune performance of macrophages, thereby improving the anti-tumor ability (Liu et al., 2020). In addition,

anti-tumor clinical trials showed that plant polysaccharides are beneficial in relieving immunosuppression, enhancing the immune response, and inhibiting tumor growth, invasion, and metastasis, as well as exerting less cytotoxicity (Kiddane & Kim, 2020).

Lycium barbarum, a member of the Solanaceae family, is a traditional Chinese medicinal herb. Its fruit can be used in soups, porridge, wine, and juice, as a dietary source of fruit (He et al., 2012). In addition, the fruit is used as a nutritional supplement in Western countries (Zhang et al., 2005). According to the traditional medical monographs, "Compendium of Materia Medica" and "Chinese Pharmacopoeia", the *Lycium barbarum* fruit possesses many biological functions, such as protection of the liver, tonification of the kidneys, moistening of the lungs, and improvement of the eyesight. Pharmacological studies showed that the *Lycium barbarum* fruit has many health-promoting properties (Feng et al., 2021), including immunomodulation, anti-aging, anti-fatigue, anti-inflammation, inhibition of cancer cell growth, as well as prevention of cardiovascular diseases, diabetes, and Alzheimer's disease, with polysaccharide as the main active component (Potterat, 2010; Tian

* Corresponding author. Lanzhou Institute of Chemical Physics, Chinese Academy of Sciences, Lanzhou, Gansu, 730000, China.

** Corresponding author.

E-mail addresses: jfliu@licp.cas.cn (J. Liu), didl@licp.cas.cn (D. Di).

¹ These authors contributed equally to this work.

et al., 2019; Zhang et al., 2005).

The majority of the studies on *Lycium barbarum* focused on the biological properties of crude *Lycium barbarum* polysaccharide (LBP). The composition of the crude polysaccharide is complex, and its physical and chemical properties, as well as its structure, are easily affected by the source and extraction process, resulting in low repeatability of the biological activity. Therefore, the extraction, separation, and purification procedures of LBP are critical (Hao et al., 2020; Zhou et al., 2020). The polysaccharide components of the *Lycium barbarum* fruit obtained through column chromatography have a low yield, restricting further research on the structure-activity relationship of LBP. However, the separation and purification of the *Lycium barbarum* fruit through ethanol fractionation precipitation increases the yield of the polysaccharide components without affecting their physical and chemical properties (Gong et al., 2018).

Previous studies showed that crude LBP inhibits the growth of cancer cells. However, the main effective components have yet to be determined. This study aimed to further systematically examine the biological properties of the *Lycium barbarum* fruit polysaccharide and determine its main effective components (Gong et al., 2020; Tang et al., 2012). Therefore, the ethanol fractionation precipitation method was used to separate and purify the *Lycium barbarum* fruit polysaccharide as well as to obtain all the crude polysaccharide components. Their effects on the growth of cancer cells were evaluated and compared, then, the polysaccharide components with high activity were further isolated and purified to further investigate their inhibitory mechanism and structure characterization. These findings might be useful for further studies on the structure-activity relationship of LBP and functional food development.

2. Materials and methods

2.1. Materials and reagents

The *Lycium barbarum* fruit was obtained from the Ningxia Hui Autonomous Region, China. Human lung adenocarcinoma cells (A549, H460, and H1975), human liver cancer cells (HepG2), human cervical cancer cells (HeLa), human gastric cancer cells (MKN-45, BGC-823, MKN-28 and SGC-7901) and human breast cancer cells (MCF-7) were obtained from the Translational Medicine Center of the Gansu Provincial Cancer Hospital. The primary antibody was purchased from Proteintech (USA). DMEM culture medium, fetal bovine serum, secondary antibody, and pancreatin were purchased from Gibco (USA). The MTT kit, cell cycle kit, Giemsa staining solution, and *Polyporus umbellatus* polysaccharide standards were purchased from Solarbio Science & Technology Co. Ltd (China) and the apoptosis kit was purchased from BD (USA).

2.2. Separation and purification of LBPs

The *Lycium barbarum* fruits were crushed, defatted, and decolorized with petroleum ether before being filtrated. The dregs were then soaked in cold water and subjected to flash extraction, followed by extraction with hot water under reflux. After filtration, absolute ethanol was added to the filtrate to obtain the concentrations of 40%, 50%, 60%, and 70% to perform step-by-step alcohol precipitation. Deproteinization, decolorization, dialysis, concentration, and freeze-drying were then performed to obtain the crude LBP (Gong et al., 2018).

2.3. Detection of cancer cell activity

Cells were cultured in DMEM containing 10% FBS in an incubator at 37 °C with 5% CO₂. Next, cancer cells were treated with different alcohol-precipitated LBPs at 1 mg/mL for 48 h. The MTT method (Gong et al., 2018) was used to determine the viability of each cancer cell line and crude LBPs and their inhibitory effect on cancer cells was evaluated.

2.4. Screening of homogeneous polysaccharide components in LBP with anti-cancer properties

After the screening, human lung cancer A549 cells were selected for the subsequent experiment. The 60% LBP was washed sequentially with distilled water, 0.2 and 0.4 M NaCl at a flow rate of 0.5 mL/min, and three fractions were obtained, defined as LBP1, LBP2, and LBP3. The main fraction was LBP1, as it was the main component, accounting for 60% of the total LBP, and it was further fractionated by gel permeation using a sephadex G-100 column. Then, it was dialyzed and lyophilized for subsequent studies (Ma et al., 2018). A549 cells were treated with the homogeneous polysaccharide components (LBP, LBP-1, LBP-2, and LBP-3) at a concentration of 1 mg/mL for 48 h. The proliferation activity of A549 cells was determined using the MTT (Gong et al., 2018) assay to evaluate which LBPs could inhibit their proliferation.

2.5. Concentration and time-dependent analysis of LBPs on A549 cells

The A549 cells were treated with LBP, LBP-1, and *Polyporus umbellatus* polysaccharide at different concentrations, such as 20 µg/mL, 50 µg/mL, 100 µg/mL, 200 µg/mL, 400 µg/mL, 800 µg/mL and 1600 µg/mL for 24 h and 48 h. The viability of A549 cells was then detected using the MTT assay (Gong et al., 2018) to determine the optimum concentrations of LBPs and PUPS.

2.6. Colony formation and wound healing assay for cell migration

The A549 cells were treated with 50 µg/mL LBP-1 and 15 µg/mL PUPS, and sensitive cells were selected for colony formation analysis according to Liu et al. (Liu et al., 2017). The ability of LBP-1 to inhibit the migration of A549 cells was determined using the method by Zhu et al. (Zhu et al., 2020).

2.7. Detection of apoptosis

A549 cells were treated with 50 µg/mL LBP-1 for 24 h, 48 h, and 72 h, then the cells were collected according to the manufacturer's instructions of the apoptosis detection kit (BD, USA), and labeled with PI and Annexin V-FITC. Apoptosis was detected and analyzed using the FACS Calibur (BD Biosciences, USA).

2.8. Cell cycle detection

A549 cells were treated with LBP-1 at the concentrations of 20 µg/mL, 50 µg/mL, and 100 µg/mL for 24 h. Then, the cells were collected according to the manufacturer's instructions of the cell cycle detection kit (Solarbio, China), and the DNA in the nuclei was labeled with PI. The cell cycle distribution was determined using the FACS Calibur (BD Biosciences, USA).

2.9. Western blot analysis

The whole-cell lysis buffer (Solarbio, China) was used to extract the whole-cell proteins, and protein concentration was determined. The extracted proteins were subjected to electrophoretic separation using sodium dodecyl sulfate-polyacrylamide gel electrophoresis. After electrotransfer to the polyvinylidene fluoride membrane, the membrane was sealed with 5% skim milk, and incubated with the following primary antibodies: PI3K (1:1000, Proteintech, USA); Phospho-PI3K (1:500, ProteinTech, USA); Akt (1:1000, Abcam, USA); Phospho-Akt (1:200, Cell Signaling Technology, USA); mTOR (1:1000, Abcam, USA); Phospho-mTOR (1:1000, ABCAM, USA); Caspase 3 (1:500, Proteintech, USA); Bax (1:500, Proteintech, USA); Bcl-2 (1:500, Proteintech, USA); Cyclin D1 (1:500, Proteintech, the USA); CDK2 (1: 500, Protentech, USA); and Cyclin D3 (1:500, Proteintech, USA). Next, the samples were incubated with a secondary antibody (1:10000, Proteintech, USA). The bands were

visualized using the Pierce® ECL protein imprinting substrate (Thermo Fisher Scientific, USA). The signals were detected using the protein blotting detection system ChemiDoc™ XRS (Bio-rad, USA).

2.10. Molecular weight distribution

The average molecular weight distribution of LBP-1 was analyzed using high-performance gel permeation chromatography (HPGPC). The following conditions were used: the sample concentration was 5 mg/mL; the mobile phase was 1 mL/min ultrapure water; the injection volume was 100 µL (Lv et al., 2013).

2.11. Monosaccharide composition analysis (ion chromatography)

The monosaccharide composition of LBP-1 was determined using ion chromatography (ICS). In this experiment, Fuc, Rha, Ara, Gal, Glc, Xyl, Man, Fru, Rib, Gal-UA, Gul-UA, Glc-UA, and Man-UA were used as the monosaccharide standards. The monosaccharide composition of LBP-1 was determined by comparing the retention time of different monosaccharide standards with the corresponding peak area and response factor of the standard monosaccharides (Kenneth Mopper et al., 1992).

2.12. Methylation analysis

Methylation analysis was carried out on LBP-1. A total of 5 mg (± 0.05 mg) polysaccharide sample was weighed, a TFA acid solution just prepared was added, then the mixture was heated at 121 °C for 2 h. Nitrogen was used for drying the sample, which was cleaned with methanol, dried, and cleaned with methanol 2–3 times again. Next, the sample was dissolved in sterile water and transferred to a chromatographic bottle. The chromatographic system used was the Thermo ICS5000+ ion chromatographic system (ICS5000+, (ThermoFisher scientific, the USA), while the liquid chromatography column used was the Dionex™ CarboPac™ PA10 (250 × 4.0 mm², 10 mm). The injection volume was 5 µL. The mobile phase A was H₂O, and the mobile phase B was 100 mM NaOH with a column temperature of 30 °C. The monosaccharide components were analyzed using an electrochemical detector (Ciucanu I, 1984).

2.13. Nuclear magnetic resonance (NMR) analysis

The dried LBP-1 sample (60 mg) was dissolved in D₂O for NMR analysis. ¹H and ¹³C NMR spectra were recorded using a 600 spectrometer.

2.14. Statistical analysis

Statistical analysis was performed using SPSS22 and the test results were expressed as ($X \pm S$). Three parallel experiments were performed, and ANOVA was adopted for Duncan multiple comparisons. A value of $P < 0.05$ was considered statistically significant.

3. Results and analysis

3.1. Determination of cancer cell viability

At present, studies on the inhibition of cancer cell growth by *Lycium barbarum* polysaccharides mainly focus on the use of crude polysaccharides and one cell line. The physicochemical properties and structures of polysaccharides change with the different extraction methods of polysaccharides, thus exerting different tumor suppressive effects. (Zhang et al., 2005). For example, Zhang et al. found that the crude polysaccharide of wolfberry fruit can significantly inhibit the growth of human hepatoma cell QGY7703 (De La Cena et al., 2021). In this study, four crude LBPs (40%, 50%, 60%, and 70% LBP) were isolated and extracted from the *Lycium barbarum* fruit by fractional alcohol

precipitation. The effects of these four crude polysaccharide components on the growth of ten common cancer cell lines were detected using the MTT assay, as shown in Fig. 1A. The results demonstrated that LBPs extracted with different alcohol precipitation concentrations had different inhibitory effects on the ten cancer cell lines, and the inhibitory effects were also different among the different cancer cells. The inhibitory effect of 60% alcohol-precipitated LBP on human lung adenocarcinoma cell A549 was significantly higher than that exerted on the other cancer cell lines. A higher inhibitory effect by 70% alcohol-precipitated LBP was observed on HeLa cells and MCF-7 cells compared to the effect on the other cancer cells. The inhibition rate of the other LBPs on cancer cells was lower than 50%, indicating that the polysaccharides had no evident inhibitory effect on cancer cells. This might be due to spontaneous apoptosis. Therefore, LBPs precipitated by different alcohol concentrations inhibited cancer cells in a specific manner. In this study, A549 cells were subsequently used to further evaluate the mechanism of action of 60% LBP (followed by LBP).

3.2. Effect of different LBP components on the proliferation of A549 cells

Three uniform LBP components (LBP-1~LBP-3) were isolated and purified from LBP. The inhibitory effect of the different LBP components on the proliferation of A549 cells was determined using the MTT assay. The results in Fig. 1B suggested that LBP and LBP-1 could significantly inhibit the proliferation of A549 cells ($P < 0.01$). Therefore, the LBP-1 component played a critical role in inhibiting cell proliferation.

3.3. Concentration and time-dependent analysis of LBP-1 on A549 cells

The inhibitory rate of the LBP solution on A549 cells gradually increased with increasing concentrations and time, as shown in Fig. 1C and D. The IC₅₀ values of the treatment with the polysaccharide component for 48 h showed that the inhibitory rate of the polysaccharide components on A549 was consistently higher than 50% when the concentrations of LBP and LBP-1 were higher than 700 µg/mL and 42.5 µg/mL. This result indicated that the optimum inhibitory effect of the polysaccharide components on A549 cells was achieved at the above concentrations. As *Polyporus umbellatus* polysaccharide has been previously used in the treatment of lung cancer, it was used as a positive control in this study (Guo et al., 2019). The treatment of A549 cells with *Polyporus umbellatus* polysaccharide resulted in a significant inhibition of A549 cell growth. The inhibitory effect of *Polyporus umbellatus* polysaccharide on human lung cancer cells gradually increased with increasing drug concentrations and time. The IC₅₀ value of lung cancer cells treated with drugs for 48 h showed that the A549 cells were sensitive to *Polyporus umbellatus* polysaccharides. The inhibitory rate of the proliferation of A549 cells treated with 42.5 µg/mL LBP-1 was equivalent to that of 15 µg/mL *Polyporus umbellatus* polysaccharide on A549 cells in comparison with the inhibitory rate exerted by LBP-1.

3.4. Inhibition of A549 cells growth by LBP-1

The healing ability of A549 cells decreased ($P < 0.01$) (Fig. 2A and B) after treating A549 cells with LBP-1 and PUPS for 24 h and 48 h, respectively. The colony formation experiment results illustrated that LBP-1 and PUPS inhibited the growth of the A549 cell colonies (Fig. 2C). Therefore, LBP-1 could inhibit the growth of A549 cells.

3.5. Promotion of A549 cell apoptosis by LBP-1

Apoptosis is one of the main mechanisms that inhibit cell growth (Sun et al., 2016). Thus, the apoptosis of A549 cells treated with LBP-1 was analyzed by flow cytometry to verify that LBP-1 plays a role in inhibiting the growth of A549 cells by inducing apoptosis. The flow cytometry results suggested that spontaneous apoptosis of untreated A549 cells was 6.85% in the early stage and 2.03% in the late stage.

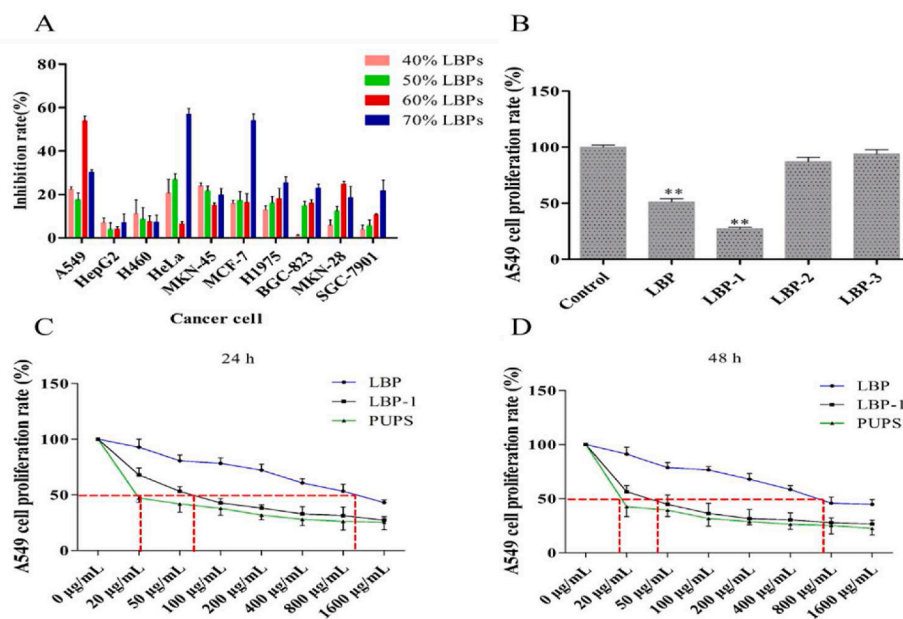


Fig. 1. Effect of *Lycium barbarum* polysaccharide components on the proliferation of cancer cells. A: effect of alcohol-precipitated crude polysaccharide components on the proliferation of cancer cells; B: effect of LBP components on the proliferation of A549 cell; C/D: effect of LBP-1 on the proliferation of A549 cells after incubation for 24 h and 48 h $**P < 0.01$.

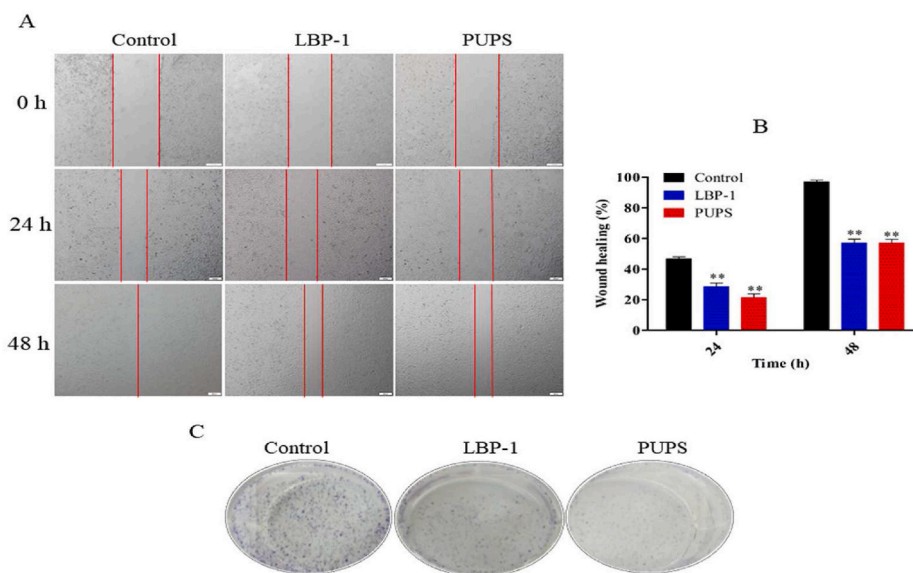


Fig. 2. Effect of LBP-1 on the growth of A549 cells. A/B: A549 colony formation experiment; C: experiment on the migration ability of A549 cells. $**P < 0.01$.

When cells were treated with 50 $\mu\text{g}/\text{mL}$ LBP-1 for 24 h, 48 h, and 72 h, the apoptotic rates in the early stage were 14.47%, 19.87%, and 18.34%, respectively, while the apoptotic rates in the late stage were 4.31%, 6.34%, and 19.93%, respectively. The apoptotic rate was significantly increased in the treated groups compared to the control group ($P < 0.05$) (Fig. 3A and B). Therefore, LBP-1 could promote apoptosis of A549 cells.

Activation of the caspase cascade of the caspase family of proteases plays an important role in various apoptotic responses (Li et al., 2012). The Bcl-2 protein family consists of anti-apoptotic and pro-apoptotic factors that play a key role in regulating cell death through apoptosis (Sun et al., 2012). The mechanism of LBP-1-induced apoptosis in A549 cells was determined by evaluating the expression of Bcl-2/Bax and caspase-3. Western blot showed that both LBP and LBP-1 promoted the expression of cleaved-caspase3 and Bax protein in A549 cells ($P < 0.05$) while they inhibited the expression of Bcl-2 ($P < 0.05$). The expression of

the apoptosis-related proteins cleaved-caspase3 and Bax in the LBP-1 group were significantly increased compared to the LBP group, the expression of Bcl-2 was significantly decreased ($P < 0.05$) (Fig. 3C and D). Therefore, LBP-1 could promote the apoptosis of A549 cells.

3.6. Induction of cell cycle arrest in A549 cells by LBP-1

The cell cycle is an important process in cell proliferation and differentiation, and it is also the basis for the unlimited proliferation of tumor cells (De La Cena et al., 2021). The cell cycle of A549 cells treated with LBP-1 was analyzed using flow cytometry. The relative percentage ratio of sub-G0/G1 increased with increasing LBP-1 concentrations, while the relative percentage of sub S decreased, as shown in Fig. 4A and B. The percentages of sub G0/G1, S, and G2/M at 100 $\mu\text{g}/\text{mL}$ were 59.48%, 36.97%, and 3.55%, respectively, indicating that LBP-1

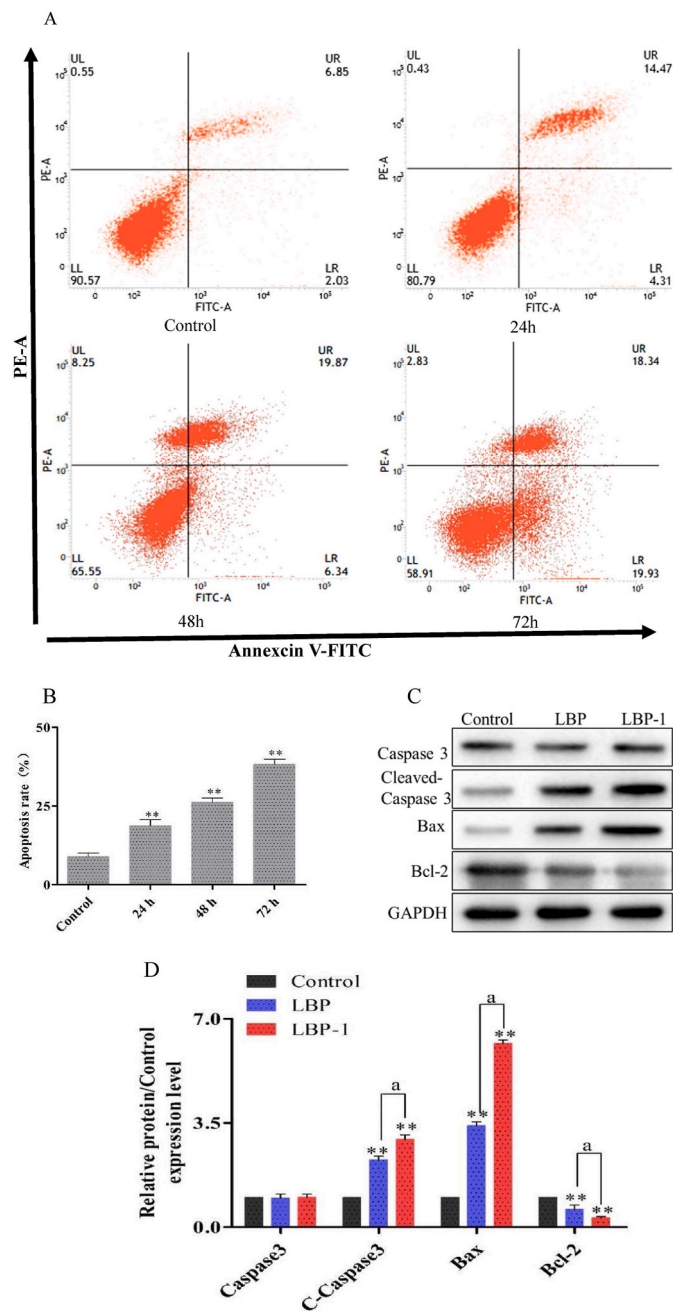


Fig. 3. Effect of LBP-1 on the apoptosis of A549 cells. A/B: apoptosis of A549 cells detected by flow cytometry; C/D: effect of LBP-1 on the expression of caspase3-3, Bax, and Bcl-2 in A549 cells. ^a*P* < 0.05, ^{**}*P* < 0.01.

blocked the cell cycle of A549 cells in the G0/G1 phase.

When cells undergo normal mitosis, cycle-related proteins such as cyclin-dependent kinase 2 (CDK2), cyclin E1 (Cyclin E1) and cyclin D1 (Cyclin D1) are involved. The main function of a positive regulator of mitosis is to regulate the G1/S transition of the cell cycle. If Cyclin D1 is abnormally overexpressed in the cells, it may lead to uncontrolled cell growth, leading to tumorigenesis (De La Cena et al., 2021). The expression of cell cycle-related proteins in A549 cells treated with LBP-I was detected using Western blot. The treatment with LBP and LBP-1 reduced the expression of Cyclin D1, CDK2, and Cyclin D3 in A549 cells (*P* < 0.01), as shown in Fig. 4C and D. A significant difference (*P* < 0.05) was observed in the expression of Cyclin D1, CDK2, and Cyclin D3 in the LBP-1 group compared to their expression in the LBP group. Therefore, LBP-1 could cause the abnormal expression of cyclins in A549 cells,

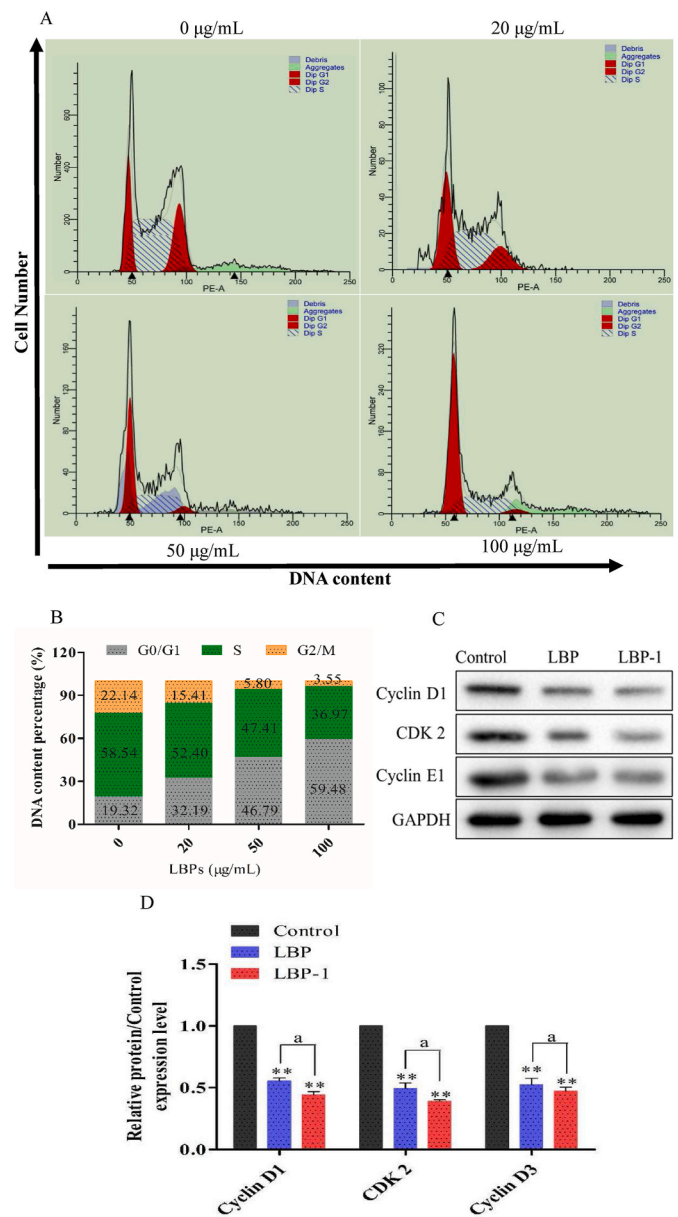


Fig. 4. Effect of LBP-1 on A549 cell cycle. A/B: cell cycle distribution results; C: effect of LBP-1 on the expression of Cyclin D1, CDK2, and Cyclin D3 in A549 cells; D: relative quantitative analysis of Cyclin D1, CDK2, and Cyclin D3 protein expression; Mean ± standard deviation, ^{**}*P* < 0.01 compared to the control group; ^a*P* < 0.05 compared to the LBP-1 group.

effectively blocking normal mitosis.

3.7. Inhibition of the activation of the PI3K/Akt/mTOR signaling pathway by LBP-1

The PI3K/Akt/mTOR signaling pathway is a classical anti-apoptotic signal transduction pathway that promotes proliferation, differentiation, and survival. Thus, the phosphorylation of PI3K/Akt/mTOR (PI3K, Akt, and mTOR) was determined in order to study the effect of LBP-1 on the PI3K/Akt/mTOR pathway in A549 cells. Fig. 5 shows that the expression of P-PI3K, P-Akt, and P-mTOR protein was down-regulated after A549 cells were treated with LBP and LBP-1 (*P* < 0.01). Therefore, LBP-1 could inhibit the activation of the PI3K/Akt/mTOR signaling pathway.

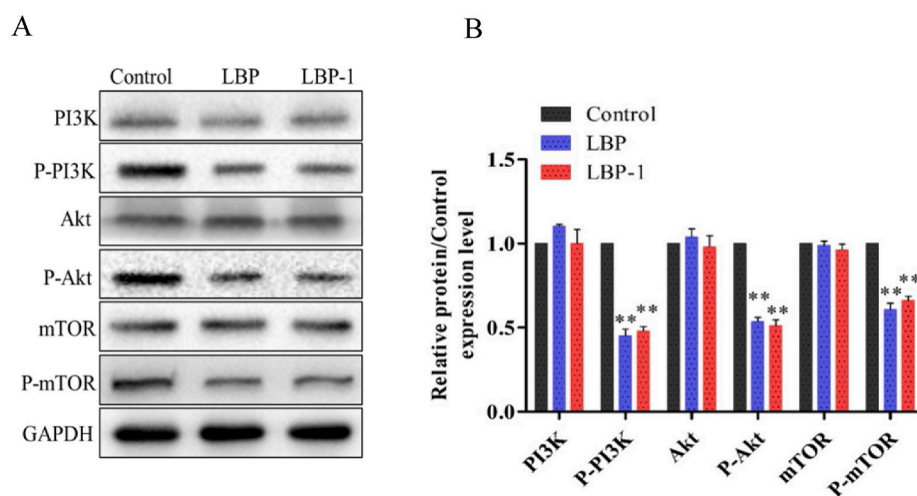


Fig. 5. Effect of LBP-1 on the PI3K/Akt/mTOR signaling pathway. A: expression of PI3K, Akt, and mTOR proteins of the PI3K/Akt/mTOR signal pathway; B: relative quantitative analysis of PI3K, Akt, and mTOR protein expression; Mean \pm SD, $^{***}P < 0.01$ compared to the control group.

3.8. Molecular weight distribution

The Mw and Mn of LBP-1 were determined as 307.8 kDa and 35.8 kDa, respectively, and the MW/Mn (polydispersity index) was 8.598.

3.9. Monosaccharide composition analysis

The monosaccharide composition of LBP-1 was analyzed using ion chromatography (ICS). LBP-1 was mainly composed of arabinose (Ara), galactose (Gal), glucose (Glc), xylose (Xyl), and mannose (Man), with molar ratios of 37.53: 28.08: 14.72: 7.83: 4.50, respectively, as shown in Table 1 and Fig. 6. Ara was the major monosaccharide in LBP-1.

3.10. Methylation and gas chromatography-mass spectrometry (GC-MS) analysis

The whole structure of LBP-1 was analyzed using methylation and GC-MS. LBP-1 and its reduction products were methylated and acetylated, then analyzed by GC-MS. The esterified arabinose accounted for approximately 50.54% of the total polysaccharide, which was consistent with the results of the monosaccharide composition, as shown in Table 1 and Fig. 7. Arabinose was used as a linking group to form arabinose groups through the t, 2, 3, and 5 glycosidic bonds. Galactose was used as

Table 1
Methylation analysis data of LBP-1.

Methylation	Connection method	Relative molar ratio (%)
1,4-di-O-acetyl-2,3,5-tri-O-methyl arabinitol	t-Ara(f)	17.319
1,5-di-O-acetyl-2,3,4-tri-O-methyl xylitol	t-Xyl(p)	4.325
1,5-di-O-acetyl-2,3,4,6-tetra-O-methyl glucitol	t-Glc(p)	3.526
1,5-di-O-acetyl-2,3,4,6-tetra-O-methyl galactitol	t-Gal(p)	5.525
1,2,5-tri-O-acetyl-3,4-di-O-methyl xylitol	2-Xyl(p)	3.110
1,3,4,5-tetra-O-acetyl-2-O-methyl arabinitol	2,3,5-Ara(f)	33.221
1,4,5-tri-O-acetyl-2,3,6-tri-O-methyl glucitol	2,4-Glc(p)	5.865
1,4,5,6-tetra-O-acetyl-2,3-di-O-methyl mannitol	2,4,6-Man(p)	2.527
1,4,5,6-tetra-O-acetyl-2,3-di-O-methyl galactitol	3,4,6-Gal(p)	24.399
1,2,3,4,5-penta-O-acetyl xylitol	Xylitol/2,3,4	0.183

a linking group to form galactose through the t, 3, 4, and 6 glycosidic bonds. Glucose, as a linking group, was bonded through the t, 2, and 4 glycosidic bonds to form a glucosyl group. Xylose, as a linking group, was linked through the t, 2, 3, and 4 glycosidic bonds to form xylose groups. Mannose was used as a linking group to form mannosyl through the t, 2, 4, and 6 glycosidic bonds.

3.11. NMR analysis

All glycosidic bond signals were attributed to a combination of heteronuclear multiple bond correlation (HMBC) and Nuclear Overhauser Effect spectroscopy (NOESY), as shown in Table 2.

The analysis based on HMBC and NOESY is shown in Fig. 8A and B. The anomeric hydrogen of $\rightarrow 5\text{-}\alpha\text{-L-Ara}(1\rightarrow$ had a related signal peak with its own C5, which verified that $\rightarrow 5\text{-}\alpha\text{-L-Ara}(1\rightarrow$ existed in the polysaccharide; the anomeric carbon of $\rightarrow 5\text{-}\alpha\text{-L-Ara}(1\rightarrow$ had a correlated signal peak with H3 of $\rightarrow 3, 6)\text{-}\beta\text{-D-Galp}(1\rightarrow$, indicating the existence of $\rightarrow 5\text{-}\alpha\text{-L-Ara}(1\rightarrow 3, 6)\text{-}\beta\text{-D-Galp}(1\rightarrow$; the anomeric carbon of $\rightarrow 5\text{-}\alpha\text{-L-Ara}(1\rightarrow$ had a correlated signal peak with H6 of $\rightarrow 6)\text{-}\beta\text{-D-Galp}(1\rightarrow$, indicating the existence of $\rightarrow 5\text{-}\alpha\text{-L-Ara}(1\rightarrow 6)\text{-}\beta\text{-D-Galp}(1\rightarrow$; the anomeric carbon of $\rightarrow 6)\text{-}\beta\text{-D-Galp}(1\rightarrow$ had a correlated signal peak with H4 of $\rightarrow 4, 6)\text{-}\beta\text{-D-Galp}(1\rightarrow$, indicating the existence of $\rightarrow 6)\text{-}\beta\text{-D-Galp}(1\rightarrow 4, 6)\text{-}\beta\text{-D-Galp}(1\rightarrow$; the anomeric carbon of $\rightarrow 3)\text{-}\beta\text{-D-Galp}(1\rightarrow$ had a correlated signal peak with H6 of $\rightarrow 3, 6)\text{-}\beta\text{-D-Galp}(1\rightarrow$, indicating the existence of $\rightarrow 3)\text{-}\beta\text{-D-Galp}(1\rightarrow 3, 6)\text{-}\beta\text{-D-Galp}(1\rightarrow$; the anomeric carbon of $\alpha\text{-L-Ara}(1\rightarrow$ had a correlated signal peak with H5 of $\rightarrow 5\text{-}\alpha\text{-L-Ara}(1\rightarrow$, indicating the existence of $\alpha\text{-L-Ara}(1\rightarrow 5\text{-}\alpha\text{-L-Ara}(1\rightarrow$; the anomeric carbon of $\alpha\text{-L-Ara}(1\rightarrow$ had a correlated signal peak with H3 of $\rightarrow 3)\text{-}\beta\text{-D-Galp}(1\rightarrow$, indicating the existence of $\alpha\text{-L-Ara}(1\rightarrow 3)\text{-}\beta\text{-D-Galp}(1\rightarrow$; the anomeric carbon of $\rightarrow 3, 6)\text{-}\beta\text{-D-Galp}(1\rightarrow$ had a correlated signal peak with H4 of $\rightarrow 4)\text{-}\alpha\text{-D-Glcp}(1\rightarrow$, indicating the existence of $\rightarrow 3, 6)\text{-}\beta\text{-D-Galp}(1\rightarrow 4)\text{-}\alpha\text{-D-Glcp}(1\rightarrow$; the anomeric carbon of $\rightarrow 3)\text{-}\beta\text{-D-Galp}(1\rightarrow$ had a correlated signal peak with H6 of $\rightarrow 4, 6)\text{-}\beta\text{-D-Galp}(1\rightarrow$, indicating the existence of $\rightarrow 3)\text{-}\beta\text{-D-Galp}(1\rightarrow 6, 4)\text{-}\beta\text{-D-Galp}(1\rightarrow$. In summary, the polysaccharide chain of LBP-1 was obtained, as shown in Fig. 8C.

4. Discussion

The biological activity of polysaccharides is closely related to their monosaccharide composition, molecular weight and type of glycosidic bonds (Sun et al., 2016). Kashimoto and Li et al. found that different water-soluble *Lycium barbarum* polysaccharide fractions can be obtained by ion exchange and size exclusion column chromatography, and among

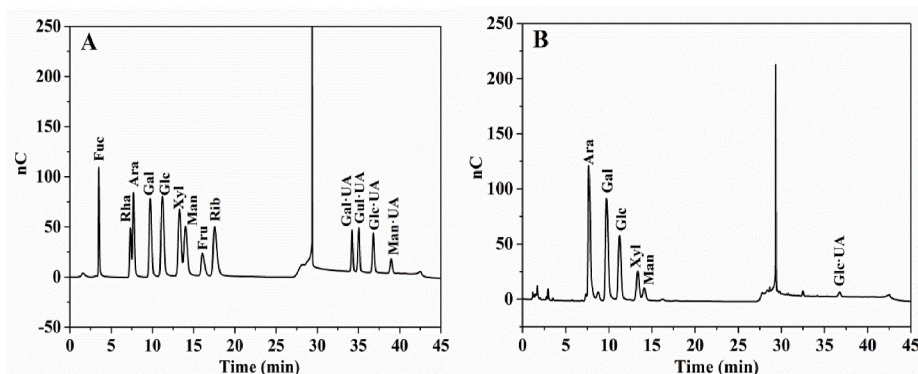


Fig. 6. Monosaccharide composition spectrum of LBP-1, A: ion chromatogram of the standard sample; B: ion chromatogram of the LBP-1 monosaccharide.

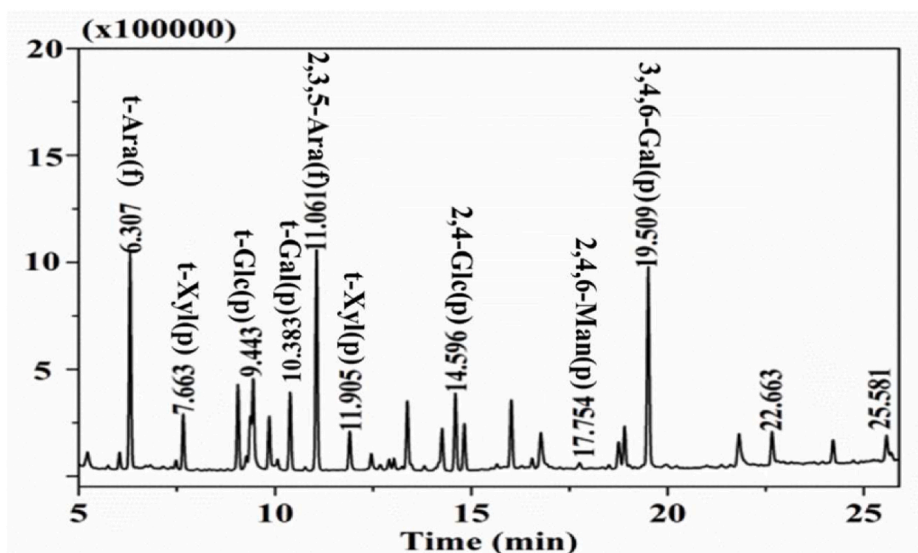


Fig. 7. Total ion flow diagram of LBP-1 monosaccharide.

Table 2
Hydrogen and carbon signals in LBP-1.

Glycosyl residues	H1/C1	H2/C2	H3/C3	H4/C4	H5/C5	H6a,b/C6
α -L-Ara(1 \rightarrow)	5.14	4.12	3.86	4.03	3.7	3.61
β -D-Galp-(1 \rightarrow)	4.36	3.61	3.93	3.78	4.03	3.7
\rightarrow 3,6)- β -D-Galp-(1 \rightarrow)	103.9	71.11	73.86	74.96	69.88	62.52
\rightarrow 5)- α -L-Ara(1 \rightarrow)	4.5	3.7	4.03	4.2	3.7	3.61
\rightarrow 4,6)- β -D-Galp-(1 \rightarrow)	105.61	69.74	83.54	71.11	69.24	64.41
\rightarrow 4)- α -D-Glcp-(1 \rightarrow)	5.08	4.12	3.93	4.03	3.47	4.03
\rightarrow 6)- β -D-Galp-(1 \rightarrow)	108.7	83.26	77.58	85.24	64.33	
\rightarrow 3)- β -D-Galp-(1 \rightarrow)	4.36	3.17	3.47	3.61	3.86	3.74
\rightarrow 4)- β -D-Galp-(1 \rightarrow)	104.4	73.85	74.96	71.34	69.74	67.29
\rightarrow 6)- β -D-Galp-(1 \rightarrow)	5.29	3.61	3.86	3.61	3.78	3.84
\rightarrow 3)- β -D-Galp-(1 \rightarrow)	100.7	73.08	74.56	78.92	72.62	61.74
\rightarrow 4)- β -D-Galp-(1 \rightarrow)	4.41	3.61	3.78	4.03	3.86	4.12
\rightarrow 3)- β -D-Galp-(1 \rightarrow)	104.64	71.98	73.86	69.88	74.56	65.34
\rightarrow 4)- β -D-Galp-(1 \rightarrow)	4.48	3.59	3.78	3.82	3.73	4.05
\rightarrow 3)- β -D-Galp-(1 \rightarrow)	103.4	71.0	82.7	69.3	75.9	61.8

them, the one with the largest molecular weight has the strongest inhibitory effect on cancer cell growth. Moreover, the study found that the composition and molecular weight of monosaccharides exert a different inhibition on cancer cell growth. The molecular weight and glycosidic bond type of polysaccharides are closely related to the inhibition of cancer cell growth (Li et al., 2012; Sun et al., 2012). In this study, LBPs were isolated using ethanol fractional precipitation and molecular sieve column chromatography to obtain uniform polysaccharide components with different molecular weights and polysaccharide composition. Next, the inhibitory effect of these polysaccharide components on the growth of cancer cells was compared. The results showed that LBP-1, a homogeneous component of LBP precipitated by 60% alcohol, promoted apoptosis and arrested the cell cycle through the inhibition of the PI3K/Akt/mTOR signaling pathway, which also inhibited cell migration and subsequently the growth and proliferation of human lung cancer A549 cells. The results were consistent with previous studies that focused on other natural compounds such as *Astragalus* polysaccharides and *Ganoderma lucidum* polysaccharides (Li et al., 2010; Yu et al., 2019). LBPs significantly inhibit the growth of MCF-7, and results from this study further confirmed the previous findings. In addition, crude LBPs significantly inhibit the growth of human liver cancer cell QGY7703 (Zhang et al., 2005). Our research indicated that the LBP components of the *Lycium barbarum* fruit did not affect the growth of HepG2, which could be due to the different cancer cell lines and extraction methods that were used. It was worth noting that crude LBP extracted by hot water contained

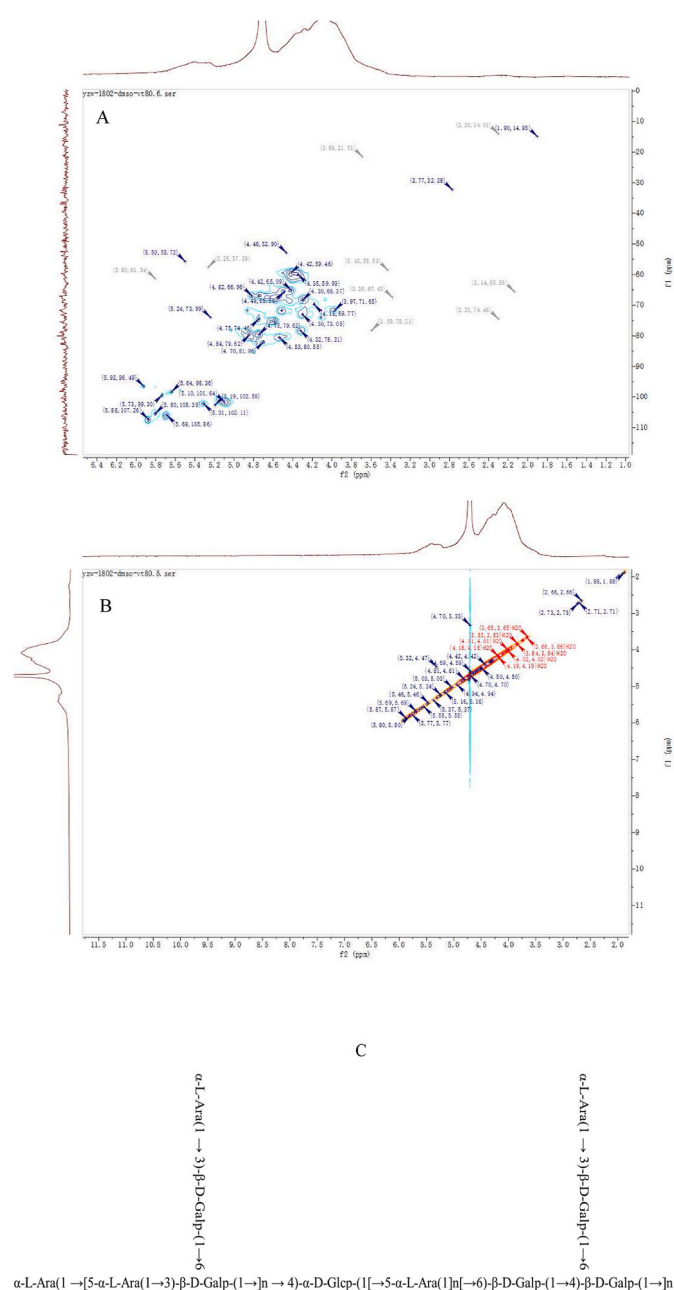


Fig. 8. NMR analysis spectra; A: HMBC spectra; B: NOESY spectra; C: chain structure of LBP-1.

uronic acid, while crude polysaccharides extracted at room temperature contained different components. Therefore, the extraction, purification, and structural characterization of LBPs could have an impact on their biological activity.

As cancer is caused by an imbalance between proliferation and apoptosis of tumor cells, apoptosis induction has emerged as a new strategy for cancer treatment. LBP, as the main active component of *Lycium barbarum* L. possesses anti-tumor properties, affecting the proliferation, apoptosis, and the cell cycle of cancer cells. Furthermore, LBP alleviates certain adverse effects of chemotherapy by boosting the body's immunity. The findings of this study also demonstrated that LBP-1 inhibited the proliferation of A549 cells while promoting apoptosis of tumor cells. Therefore, the proliferation and apoptosis of tumor cells were generally in a balanced state.

5. Conclusion

In this study, LBP-1, a homogeneous component of LBP precipitated by 60% alcohol, was selected to determine the inhibitory effect of LBP and its mechanism of action on human lung cancer cells. The findings showed that the treatment with 50 $\mu\text{g}/\text{mL}$ LBP for 24 h, 48 h, and 72 h resulted in A549 cell apoptosis rate of 18.78%, 26.21%, and 38.27%, respectively. The effect of LBP on the A549 cells cycle was determined by flow cytometry, with results showing that LBP blocked A549 cells in the G1/S phase. Thus, LBP could effectively inhibit the proliferation and migration of A549 cells. The Western blot results showed that LBP induced the abnormal expression of Cyclin D1, CDK2, and Cyclin D3, promoted the expression of caspase 3 and Bax, inhibited the expression of Bcl-2, and downregulated the expression of P-PI3K, P-Akt, and P-mTOR. Therefore, LBP-1 blocked A549 cells in the G1/S phase by inhibiting the PI3K/Akt/mTOR signaling pathway, inducing apoptosis and thereby inhibiting the growth, proliferation, and migration of A549 cells. According to the structure analysis, LBP-1 was mainly composed of Arabinose (Ara), Galactose (Gal), glucose (Glc), Xylose (Xyl), and Mannose (Man), with molar ratios of 37.53: 28.08: 14.72: 7.83: 4.50, respectively, with a molecular weight of 307.8 kDa. The primary structure of LBP-1 was obtained using NMR and methylation analysis. In conclusion, LBP-1 is a natural polysaccharide product potentially effective in the treatment of lung cancer or as a complementary drug for antitumor treatments.

Research data related to this submission

There are no linked research data sets for this submission. The reason is the following: Data are available on request.

Authors' contributions

DDL conceived and designed the experiments; ZYB, WB, LB, LJF, LML and YB performed the experiments and acquired the data, MWJ, ZYB, and LWJ analyzed the data; ZYB and LWJ drafted the manuscript; MWJ, LJF, and DDL interpreted the data and critically revised the manuscript. All authors read and approved the final version of the manuscript.

Declaration of competing interest

The authors declare that they have no conflicts of interest.

Acknowledgments

This research was funded by the Key Research and Development Program of the Ningxia Hui Autonomous Region (2021BEF02011) and the CAS "Light of West China" Program.

References

- Brody, H. (2014). Lung cancer. *Nature*, 513(7517), S1.
- Ciucanu I, K. F. (1984). A simple and rapid method for the permethylation of carbohydrates. *Carbohydrate Research*, 131(2), 209–217.
- De La Cena, K. O. C., Ho, R. X., Amraei, R., Woolf, N., Tashjian, J. Y., Zhao, Q., Richards, S., Walker, J., Huang, J., Chitalia, V. C., & Rahimi, N. (2021). Transmembrane and immunoglobulin domain containing 1, a putative tumor suppressor, induces G2/M cell cycle checkpoint Arrest in colon cancer cells. *American Journal Of Pathology*, 191(1), 157–167.
- Duma, N., Santana-Davila, R., & Molina, J. R. (2019). Non-small cell lung cancer: Epidemiology, screening, diagnosis, and treatment. *Mayo Clinic Proceedings*, 94(8), 1623–1640.
- Feng, L., Tang, N., Liu, R., Nie, R., Guo, Y., Liu, R., & Chang, M. (2021). Effects of different processing methods on bioactive substances and antioxidant properties of *Lycium barbarum* (goji berry) from China. *Food Bioscience*, 42, Article 101048.
- Gong, G., Dang, T., Deng, Y., Han, J., Zou, Z., Jing, S., Zhang, Y., Liu, Q., Huang, L., & Wang, Z. (2018). Physicochemical properties and biological activities of polysaccharides from *Lycium barbarum* prepared by fractional precipitation. *International Journal of Biological Macromolecules*, 109, 611–618.

- Gong, G., Liu, Q., Deng, Y., Dang, T., Dai, W., Liu, T., Liu, Y., Sun, J., Wang, L., Liu, Y., Sun, T., Song, S., Wang, Z., & Huang, L. (2020). Arabinogalactan derived from *Lycium barbarum* fruit inhibits cancer cell growth via cell cycle arrest and apoptosis. *International Journal of Biological Macromolecules*, *149*, 639–650.
- Guo, Z., Zang, Y., & Zhang, L. (2019). The efficacy of *Polyporus Umbellatus* polysaccharide in treating hepatitis B in China. *Progress in Molecular Biology and Translational Science*, *163*, 329–360.
- Hao, W., Wang, S. F., Zhao, J., & Li, S. P. (2020). Effects of extraction methods on immunology activity and chemical profiles of *Lycium barbarum* polysaccharides. *Journal of Pharmaceutical and Biomedical Analysis*, *185*, Article 113219.
- He, N., Yang, X., Jiao, Y., Tian, L., & Zhao, Y. (2012). Characterisation of antioxidant and antiproliferative acidic polysaccharides from Chinese wolfberry fruits. *Food Chemistry*, *133*(3), 978–989.
- Huang, W. C., Kuo, K. T., Bamodu, O. A., Lin, Y. K., Wang, C. H., Lee, K. Y., Wang, L. S., Yeh, C. T., & Tsai, J. T. (2019). Astragalus polysaccharide (PG2) ameliorates cancer symptom clusters, as well as improves quality of life in patients with metastatic disease, through modulation of the inflammatory cascade. *Cancers*, *11*(8).
- Jiao, R., Liu, Y., Gao, H., Xiao, J., & So, K. F. (2016). The anti-oxidant and antitumor properties of plant polysaccharides. *The American Journal of Chinese Medicine*, *44*(3), 463–488.
- Kenneth Mopper, C. A. S., Lionel Chevolut, t C. G., \$ Rene Revuelta, s, & Rodger, D. (1992). Determination of sugars in unconcentrated seawater and other natural waters by liquid chromatography and pulsed amperometric detection. *Environmental Science & Technology*, *26*(1), 133–138.
- Kiddane, A. T., & Kim, G. D. (2020). Anticancer and immunomodulatory effects of polysaccharides. *Nutrition and Cancer*, 1–13.
- Li, N., Hu, Y. L., He, C. X., Hu, C. J., Zhou, J., Tang, G. P., & Gao, J. Q. (2010). Preparation, characterisation and anti-tumour activity of *Ganoderma lucidum* polysaccharide nanoparticles. *Journal of Pharmacy and Pharmacology*, *62*(1), 139–144.
- Liu, C. P., Li, X., Lai, G. N., Li, J. H., Jia, W. Y., Cao, Y. Y., Xu, W. X., Tan, Q. L., Zhou, C. Y., Luo, M., Zhang, X. Y., Yuan, D. Q., Tian, J. Y., Zhang, X., & Zeng, X. (2020). Mechanisms of macrophage immunomodulatory activity induced by a new polysaccharide isolated from *polyporus umbellatus* (Pers.) fries. *Frontiers of Chemistry*, *8*, 581.
- Liu, Z., Ren, B., Wang, Y., Zou, C., Qiao, Q., Diao, Z., Mi, Y., Zhu, D., & Liu, X. (2017). Sesamol induces human hepatocellular carcinoma cells apoptosis by impairing mitochondrial function and suppressing autophagy. *Scientific Reports*, *7*, 45728.
- Li, X. L., Wang, Z. H., Zhao, Y. X., Luo, S. J., Zhang, D. W., Xiao, S. X., & Peng, Z. H. (2012). Isolation and antitumor activities of acidic polysaccharide from *Gynostemma pentaphyllum* Makino. *Carbohydrate Polymers*, *89*(3), 942–947.
- Lv, X., Wang, C., Cheng, Y., Huang, L., & Wang, Z. (2013). Isolation and structural characterization of a polysaccharide LRP4-A from *Lycium ruthenicum* Murr. *Carbohydrate Research*, *365*, 20–25.
- Ma, W., Chen, X., Wang, B., Lou, W., Chen, X., Hua, J., Sun, Y. J., Zhao, Y., & Peng, T. (2018). Characterization, antioxidativity, and anti-carcinoma activity of exopolysaccharide extract from *Rhodotorula mucilaginosa* CICC 33013. *Carbohydrate Polymers*, *181*, 768–777.
- Mattern, J., & Volm, M. (2004). Imbalance of cell proliferation and apoptosis during progression of lung carcinomas. *Anticancer Research*, *24*(6), 4243–4246.
- Pan, H., Wang, Y., Na, K., Wang, Y., Wang, L., Li, Z., Guo, C., Guo, D., & Wang, X. (2019). Autophagic flux disruption contributes to *Ganoderma lucidum* polysaccharide-induced apoptosis in human colorectal cancer cells via MAPK/ERK activation. *Cell Death & Disease*, *10*(6), 456.
- Potterat, O. (2010). Goji (*Lycium barbarum* and *L. chinense*): Phytochemistry, pharmacology and safety in the perspective of traditional uses and recent popularity. *Planta Medica*, *76*(1), 7–19.
- Sun, L., Chu, J., Sun, Z., & Chen, L. (2016). Physicochemical properties, immunomodulation and antitumor activities of polysaccharide from *Pavlova viridis*. *Life Sciences*, *144*, 156–161.
- Sun, L., Wang, L., & Zhou, Y. (2012). Immunomodulation and antitumor activities of different-molecular-weight polysaccharides from *Porphyridium cruentum*. *Carbohydrate Polymers*, *87*(2), 1206–1210.
- Tang, W. M., Chan, E., Kwok, C. Y., Lee, Y. K., Wu, J. H., Wan, C. W., Chan, R. Y., Yu, P. H., & Chan, S. W. (2012). A review of the anticancer and immunomodulatory effects of *Lycium barbarum* fruit. *Inflammopharmacology*, *20*(6), 307–314.
- Tian, X., Liang, T., Liu, Y., Ding, G., Zhang, F., & Ma, Z. (2019). Extraction, structural characterization, and biological functions of *Lycium Barbarum* polysaccharides: A review. *Biomolecules*, *9*(9).
- Yu, J., Ji, H., Yang, Z., & Liu, A. (2019). Relationship between structural properties and antitumor activity of Astragalus polysaccharides extracted with different temperatures. *International Journal of Biological Macromolecules*, *124*, 469–477.
- Zhang, M., Chen, H., Huang, J., Li, Z., Zhu, C., & Zhang, S. (2005). Effect of lycium barbarum polysaccharide on human hepatoma QGY7703 cells: Inhibition of proliferation and induction of apoptosis. *Life Sciences*, *76*(18), 2115–2124.
- Zhou, S., Rahman, A., Li, J., Wei, C., Chen, J., Linhardt, R. J., Ye, X., & Chen, S. (2020). Extraction methods affect the structure of goji (*Lycium barbarum*) polysaccharides. *Molecules*, *25*(4).
- Zhu, G., Cheng, Z., Huang, Y., Zheng, W., Yang, S., Lin, C., & Ye, J. (2020). MyD88 mediates colorectal cancer cell proliferation, migration and invasion via NFκB/AP1 signaling pathway. *International Journal of Molecular Medicine*, *45*(1), 131–140.